Appl. Phys. B 77, 421–426 (2003)
DOI: 10.1007/s00340-003-1276-6

Applied Physics B
Lasers and Optics

G. MCCARTHY[1,✉]
T. BREUNINGER[1]
J. SCHRÖDER[2]
C. DENZ[2]
D. NESHEV[3]
W. KROLIKOWSKI[1]

Mutual spatial-soliton trapping in photorefractive media: experiment versus theory

[1] CUDOS and Laser Physics Centre, Research School of Physical Sciences and Engineering, The Australian National University, Canberra, ACT 0200,Australia
[2] Institut für Angewandte Physik, Westfälische Wilhelms-Universität, Correnstrasse 2/4, 48149 Münster, Germany
[3] CUDOS and Nonlinear Physics Group, Research School of Physical Sciences and Engineering, The Australian National University, Canberra, ACT 0200, Australia

Received: 19 May 2003/Revised version: 10 July 2003
Published online: 10 September 2003 •

ABSTRACT We investigate the interaction of two-dimensional solitons propagating at small angles in a photorefractive crystal. We observe fusion of the beams when the intersecting angle is lower than some critical value. We measure the critical angle for fusion for different relative phase relations of the beams and demonstrate how this effect can be used to steer and switch the propagation of an additional optical beam.

PACS 42.65.Tg; 42.79.Ta

1 Introduction

The characteristic features of optical solitons, such as their stability, robustness, and consequent practical relevance, have been the subject of extensive studies in recent decades [1–3]. Temporal solitons are currently used to code bit signals in data streams transmitted through multi-channel telecommunication networks [4], while their spatial counterparts potentially offer important applications in all-optical processing [5] and parallel computing [6–8]. Spatial solitons (non-diffracting beams) propagating in nonlinear media can be used to form reconfigurable optical circuits – virtual circuitry created by light alone in which all-optical switching or processing is achieved through the evolution and interaction of the various soliton beams [9].

The continual interest in spatial optical solitons has been motivated to a great extent by their unique collisional properties. It appears that the majority of these properties are universal and do not depend significantly on the particular type of nonlinear model supporting the solitons [2]. From the advent of soliton physics, it has been apparent that, in many aspects, solitons behave like particles. They are robust objects displaying interaction "forces" whose nature is determined by the their relative phase and/or mutual coherence. Depending on whether they collide elastically or inelastically, solitons may either pass through each other virtually intact in the former, or fuse, be annihilated, or split in the latter case [10–13].

Soliton collisions have been observed in a variety of nonlinear media, including liquids [14–16], nonlinear glass waveguides [17], and atomic vapours [18]. An enormous boost to soliton physics, especially to its experimental endeavours, was provided by the discovery of spatial solitons in photorefractive materials [19–21]. The strong nonlinearity at extremely low optical power (microwatts) makes photorefractive materials very attractive for soliton studies. In fact, the most spectacular examples of the soliton interaction process have been achieved with photorefractive solitons, including soliton fusion, fission, and birth [22–25]. Although many experiments have demonstrated the interaction behaviour of coherent [22–24] and incoherent [25, 26] beams, no quantitative investigation of the conditions for trapping, fusion, or repulsion in terms of angular separation and relative coherence has been made up to now. Such an investigation would be indispensable for applications.

In this work we present detailed experimental and theoretical studies of the mutual self-trapping of two optical beams in a biased photorefractive crystal. We consider the interaction of two beams when they overlap at the front (input) face of the nonlinear medium, a geometry also discussed by Mamaev et al. [27]. However, in contrast with that work, which was mainly concerned with the demonstration of switching between soliton fusion and repulsion, the goal of our research is broader. By varying the crossing angle between the beams we show how the beam interaction depends on their mutual phase and coherence properties. We also discuss the applicability of these effects in soliton-based switching and show that optimal conditions exist for the crossing angle for maximal switching contrast. While experiments are performed in a specific nonlinear medium, namely a photorefractive crystal, our numerical calculations show that the results are sufficiently general to represent generic features of soliton interaction in other nonlinear systems.

2 Experimental arrangements

In our experimental realisation we consider a geometry in which two input beams overlap at the input face of the crystal (inset in Fig. 1). This geometry is chosen for two reasons. Firstly, it allows for maximal separation of the beams at the output face. Secondly, it facilitates the experimental alignment and allows for monitoring of the relative phase of the beams at the point of collision. A disadvantage is that the interaction length is effectively reduced and it requires that the

✉ Fax: +61-2/6125-0029, E-mail: glen.mccarthy@anu.edu.au

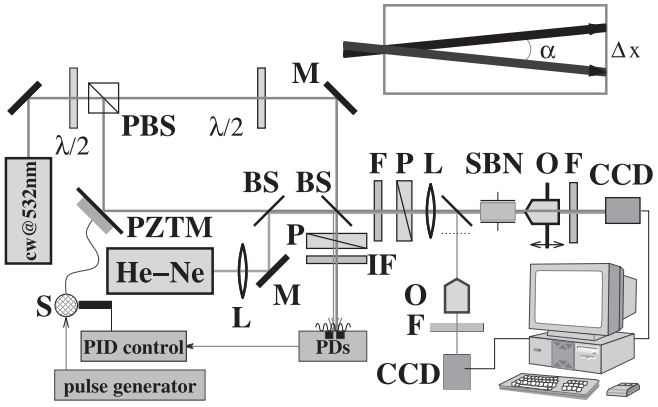

FIGURE 1 Experimental setup: PBS, polarizing beam splitter; $\lambda/2$, half-wave plate; M, mirror; BS, beam splitter; PZTM, piezoelectric transducer mirror; S, electrical switch; L, lens; P, polarizer; IF, interference filter; O, microscope objective; F, filter; SBN, photorefractive crystal; PDs, photo-diodes; CCD, camera. *Inset*: position of the two beams inside the photorefractive crystal

input beams are close to the size and shape of the actual soliton beams.

The experimental setup is shown in Fig. 1. It uses an electronic control and stabilisation of the relative phase between the two beams for accurate phase control during measurements. The beam of a green (532 nm) frequency-doubled Nd:YVO_4 laser is split in two by a polarizing beam splitter (PBS), forming the two arms of a Mach–Zehnder interferometer. The splitting ratio is controlled by a half-wave plate placed in front of the PBS, while a second half-wave plate rotates the polarization of the transmitted beam to the vertical direction. The two beams are then combined at a beam splitter and directed to the 10-mm-long photorefractive strontium barium niobate (SBN) crystal with its *c*-crystalline axis parallel to the (extraordinary) polarisation of the beams. An external biasing field is applied to the crystal along its *c*-crystalline axis (vertical direction). The (virtual) front and the (real) back faces of the crystal are simultaneously observed by two CCD cameras. The relative phase between the two beams is stabilised and controlled by monitoring the interference pattern of the two beams from the second output of the interferometer. This interference pattern is stabilised by a split-photo-detector and a proportional-integral-derivative(PID) controller. The error signal from the controller is applied to a piezoelectric-transducer mirror (PZTM) mounted in one of the interferometer arms. The PZTM could also be set to vibrate at a high frequency (~ 1 kHz), thus making both beams effectively mutually incoherent inside the crystal [28]. This is possible due to the slow time response of the crystal (~ 1 s).

Additionally, a red He-Ne beam can be made to co-propagate with one of the green beams in order to explore the guiding and switching properties of the created waveguides. The crystal is illuminated with a homogeneous white light in order to vary the dark irradiance of the crystal and subsequently to control the degree of saturation of the nonlinearity.

3 Experimental observations

The two beams are focused, with a 5-cm lens, onto the input face of the SBN crystal such that they overlap at the front face of the crystal. They interact in a horizontal plane at a small crossing angle α (see the inset of Fig. 1), while the external electric field is vertical. This orientation limits the effects of diffusion associated with the anisotropic photorefractive nonlinearity on the beam interaction, which allows for a better comparison between experiments and the theoretical model. Both input beams have equal powers of 0.44 μW and full widths half-maximum (FWHM) of 20 μm. The crystal is biased with a field of 2800 V/cm and it is illuminated with uniform white light of $\sim 80\,\mathrm{mW/cm^2}$. Under these conditions a single beam propagates without changing its initial width, therefore forming a soliton close to the input face. We measure the separation of the beams at the output face of the crystal as a function of the crossing angle (α) between the beams and their relative phase. When the double-peak structure in the output intensity distribution disappears we assume that a single beam is formed. In this case the separation between the beams is measured as zero. In Fig. 2 we present the separation curves for three different phase relations between the beams: out-of-phase, in-phase, and mutually incoherent beams.

The interaction between the beams is practically independent of the relative phase at higher angles ($> 1°$). This phase independence implies that the collision is not affected by the interaction forces due to the large transverse momentum of the beams. The beams only experience a small transverse shift from their non-perturbed positions when there is no interaction between them (dashed line in Fig. 2). This displacement is attributed to the particular interaction geometry, that is, overlapping the beams at the input face of the crystal. If the interaction process happens inside the crystal and the beams are well separated at the input, such a shift is not observed.

Decreasing the crossing angle between the beams leads to a significant difference in the interaction behaviour for the three different phase relations. The out-of-phase solitons always stay well separated at the output face of the crystal (circles in Fig. 2). This behaviour is expected since the pre-

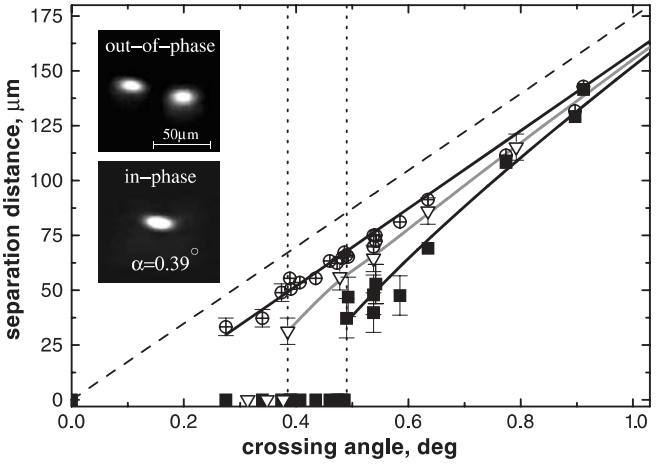

FIGURE 2 Experimentally measured separation between the solitons at the crystal output as a function of the crossing angle between them: *circles*, out-of-phase beams; *squares*, in-phase beams; *triangles*, mutually incoherent beams; *solid lines*, polynomial fits to the experimental data. The *dashed line* indicates the separation between the beams if there were no interaction between them. *Error bars* that account for the variation of the initial conditions are shown for lower crossing angles. *Inset*: images of out-of-phase collision and in-phase fusion for $\alpha = 0.39°$

dominant interaction forces are repulsive. A small vertical shift of one of the beams is observed, as seen in the inset of Fig. 2. We attribute this displacement to the inhomogeneity of the space-charge electric field inside the crystal, which induces asymmetry in the diffusion effect for each beam.

For in-phase solitons (squares in Fig. 2) and incoherent beams (triangles in Fig. 2), the interaction of the beams is attractive. It is clearly seen that this attraction leads to a decrease of the output separation between the beams with respect to the linear dependence. The collision of the in-phase soliton beams displays a threshold character leading to fusion of the two solitons for crossing angles smaller than a critical angle $\alpha_{\rm cr}$. Under our experimental conditions we measured $\alpha_{\rm cr} = 0.49°$. When fusion occurs, the two beams merge into a single elongated beam that carries almost twice the power of the individual beams. Two images of the output beams for "in-phase" and "out-of-phase" beams are shown in the inset of Fig. 2 for a crossing angle of $\alpha = 0.39°$.

In the case of incoherent collisions the interaction forces are also attractive. However the attraction is weaker compared with the in-phase solitons. This is clearly seen in Fig. 2, in which the separation distance between the beams is always greater than for the in-phase solitons. Incoherent interactions lead to beam fusion at smaller angles: $\alpha_{\rm cr} = 0.38°$ compared with 0.49° for the in-phase case.

At angles smaller than 0.27°, it was not possible to accurately measure the separation of the beams, since their interference causes a significant change of the intensity in the interacting region. This is especially valid for out-of-phase beams, for which the intensity in the interaction region becomes very low, resulting in practically no nonlinear interaction.

The critical angles for fusion are dependent on the effective nonlinearity and can vary from the particular measured values. In our case they can be changed by varying the biasing voltage on the crystal or the background illumination. However, under any conditions the general behaviour of the interaction is preserved. In particular, the strongest attraction between the beams is observed for in-phase solitons. This strong mutual attraction causes the in-phase beams to fuse at larger angles than the incoherent beams, while the out-of-phase beams always stay well separated.

4 Theoretical analysis

To support our experimental results and to provide a better insight into the dynamics of the collisions inside the crystal, we carried out numerical simulations. We consider the evolution of the electric field envelope $\boldsymbol{E}$ propagating in a biased photorefractive crystal. In our experimental arrangement the electric filed $\boldsymbol{E} = \{E_1, E_2\}$ consists of two incoherent components

$$\begin{Bmatrix} E_1 \\ E_2 \end{Bmatrix} = \begin{Bmatrix} u_1 \mathrm{e}^{-(r/w)^2 + \mathrm{i}k_x x} + u_2 \mathrm{e}^{-(r/w)^2 - \mathrm{i}k_x x} \\ u_3 \mathrm{e}^{-(r/w)^2 - \mathrm{i}k_x x} \end{Bmatrix} , \qquad (1)$$

where $r^2 = x^2 + y^2$ is the radial coordinate, w is the beam width, $k_x = (2\pi n/\lambda)\,\alpha/2$, and u_j, $j = 1...3$, are the amplitudes of the different beams. For out-of-phase beams $u_1 = -u_2$ and $u_3 = 0$. For in-phase beams $u_1 = u_2$ and $u_3 = 0$, while for incoherent beams $u_1 = u_3$ and $u_2 = 0$. The theoretical description of the beam propagation employs the Zozulya–Anderson model, which takes into account the most important properties of photorefractive nonlinearities [29, 30]. When the characteristic spatial scales are larger than the photorefractive Debye length and the diffusion field is neglected, the steady-state propagation along the z axis of the crystal with an externally applied electric field along the y axis is described by

$$\mathrm{i}\frac{\partial \boldsymbol{E}}{\partial z} + \frac{1}{2}\nabla^2 \boldsymbol{E} = -\frac{\gamma}{2}\frac{\partial \varphi}{\partial y}\boldsymbol{E} ,$$
$$\nabla^2 \varphi + \nabla\varphi \nabla \ln(1+I) = E_0 x_0 \frac{\partial}{\partial y}\ln(1+I) , \qquad (2)$$

where $\nabla = \hat{x}(\partial/\partial x) + \hat{y}(\partial/\partial y)$, and γ and E_0 are the normalized nonlinearity coefficient and external electric field, respectively. φ is the dimensionless electrostatic potential induced by the light with the boundary condition $\nabla\varphi(\vec{r} \to \infty) \to 0$. The propagation coordinate z is measured in units of the diffraction length, and the transverse coordinates are normalized by the characteristic beam size x_0.

We calculated the output separation between the beams at different relative phases, confirming the general behaviour of the interactions. The results for the output separation between the solitons as a function of the crossing angle are presented in Fig. 3a and are in good agreement with the experimental data. They clearly illustrate the threshold-type behaviour of the in-

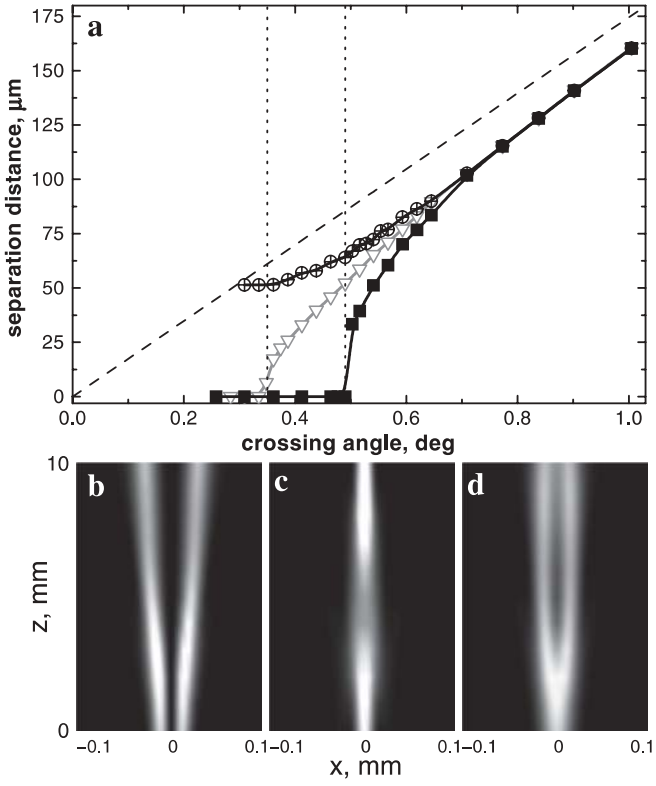

FIGURE 3 Numerical calculations for interaction of solitons in a photorefractive medium. **a** Dependence of the separation between the two beams at the output face of the crystal with respect to the crossing angle: *circles*, out-of-phase beams; *squares*, in-phase beams; *triangles*, incoherently interacting beams. The *dashed line* indicates the separation between non-interacting beams. **b–d** Contour plots displaying the beam evolution when propagating through the crystal at a crossing angle of $\alpha = 0.39°$: **b** out-of-phase; **c** in-phase; **d** incoherent beams. *White* corresponds to high intensity

teraction of in-phase and incoherent solitons, leading to fusion of the beams. In the calculations the effective dark irradiance was adjusted such that the critical angle for fusion of the in-phase beams matches the experimental value of 0.49°. The angle for fusion of incoherent solitons in this case is 0.35°, which is 10% lower than the experimentally measured value. The out-of-phase solitons exhibit a repulsive interaction and stay separated, approaching the separation for non-interaction for large crossing angles.

The presence of the optical beam in the self-focusing medium induces a refractive index change that reflects the light intensity distribution. In particular, a finite beam forms a waveguide that simultaneously guides the beam. For the initially overlapping incoherent and in-phase beams the resulting index change is largest in the centre of the light intensity distribution. As a result, both beams are directed toward this region exhibiting attraction. Fusion of the beams will take place when their crossing angle (α) is smaller than the critical angle for total internal reflection. The latter is determined by the maximum refractive index change induced by the overlapping beams. Its value can be estimated using simple geometric optics, which predict that a light ray associated with a trajectory of one of the beams will experience total internal reflection if the initial propagation angle satisfies the condition $\alpha/2 = \sqrt{2\Delta n(0)}/n$ [31]. The parameter $\Delta n(0)$ is the maximum value of the intensity-dependent refractive index change induced by the beams. Since for two identical in-phase beams the maximum intensity is two times higher than for the incoherent beams, the resulting index modulation is higher, leading to stronger attraction of the beams and a larger value of the critical angle.

The performed numerical calculations allow us to monitor the dynamics of the interaction inside the nonlinear medium. In Fig. 3b and c we show the evolution of the transverse section of the propagating beams. The out-of-phase solitons cannot trap each other and stay separated at all propagation distances. More interesting though is the dynamics of the interaction between the in-phase and incoherent beams. Due to the interaction forces, both beams may be trapped together. In the experiments the nonlinear propagation is limited, therefore we observe that below the critical angle the beams merge into a single peak state. In the calculations, on further propagation, we can actually see that this single state possesses internal oscillation modes (Fig. 3c) and its width and intensity oscillates with the propagation length.

In order to show that our results, in particular those represented by experimental measurements (Fig. 2) and numerical calculations (Fig. 3), reflect generic behavior of interacting solitons, not affected by the specific properties of the photorefractive nonlinearity, we simulated collisions of solitons described by the generalized nonlinear Schrödinger equation. For the slowly varying envelope of the electric field $\boldsymbol{E} = \{E_1, E_2\}$ it has the form

$$\mathrm{i}\frac{\partial \boldsymbol{E}}{\partial z} + \frac{1}{2}\nabla^2 \boldsymbol{E} - f(I)\boldsymbol{E} = 0\,, \tag{3}$$

where $f(I)$ is a general function dependent on the total intensity $I = \sum_m |E_m|^2$, $m = 1, 2$. In our simulations we used $f(I) \propto 1/(1+I)$, which represents typical saturable behavior of nonlinear optical media. The initial conditions for the interacting beams as well as the total nonlinear refractive index change are the same as those employed for the simulations of (1) and (2). We varied the angle between interacting solitons and measured their final separation after propagating in a 10-mm-long nonlinear medium. The results show analogous behaviour to Fig. 3 for the photorefractive nonlinearity in that the threshold for fusion is quantitatively the same and, in agreement with the earlier results and physical intuition, the fusion threshold for the in-phase coherent interaction corresponds to a higher critical angle than that of the mutually incoherent beams. Therefore it is clear that our experimental results correctly describe generic interaction properties of spatial solitons, which are independent of the particulars of the nonlinear model supporting the formation of the solitons.

The calculations for different types of nonlinearity, including Kerr-type nonlinearity, also display the decrease of the output separation between the beams (at higher crossing angles) with respect to the separation of non-interacting beams. These results confirm our earlier statement that the observed shift is a result of the particular interaction geometry. This decrease in the separation between the beams, however, tends to zero as the crossing angle is increased further.

5 Towards optical switching

The fusion of two in-phase interacting beams can possibly be implemented into a scheme for optical switching [27]. Such switching is based on the ability to control the beam interaction from repulsive to attractive by simply altering the phase of one of the beams with respect to the other one. Changing the relative phase from 0 to π results in switching between two states, for which two separated beams or one single beam is observed at the crystal output for crossing angles below the fusion threshold. The phase could be changed by increasing/decreasing the optical path for one of the beams by $\lambda/2$. Since a very small change is required for the actual switching it can be realised in many different ways. In our experiments it is achieved by inverting the error signal driving the PZT mirror.

For practical optical switching, the two states have to be clearly distinguishable. We define the contrast of the switching as the ratio of the gap between the double-peak structure of the out-of-phase beams, $\boldsymbol{G}$, to the width of the fused in-phase beams, $\boldsymbol{P}$ (inset of Fig. 4). This ratio has to be bigger than unity in order to claim switching for any practical purpose. To determine the optimal crossing angle between the beams, such that the contrast of the switching is maximal, we measured the separation between the two peaks at half of the maximum intensity, and the full width at half maximum of the fused beam. In Fig. 4 we plot the ratio between these two parameters ($\boldsymbol{G}/\boldsymbol{P}$). The experimental data are presented as points, while the results of the numerical calculations are presented with a solid line. The dashed line in Fig. 4 is the best fit to the experimental points, obtained as the ratio of the fits for the two functions $\boldsymbol{G}(\alpha)$ and $\boldsymbol{P}(\alpha)$. Though the statistical error of these measurements is rather large, there is a distinct region of angles $\alpha \in [0.35\text{–}0.45°]$ in which the ratio $\boldsymbol{G}/\boldsymbol{P}$ is higher than one. In this region a clearly pronounced single maximum exists at $\alpha = 0.4°$, for which $\boldsymbol{G}/\boldsymbol{P} \sim 2$. This region exists significantly below the critical angle, since the fused in-

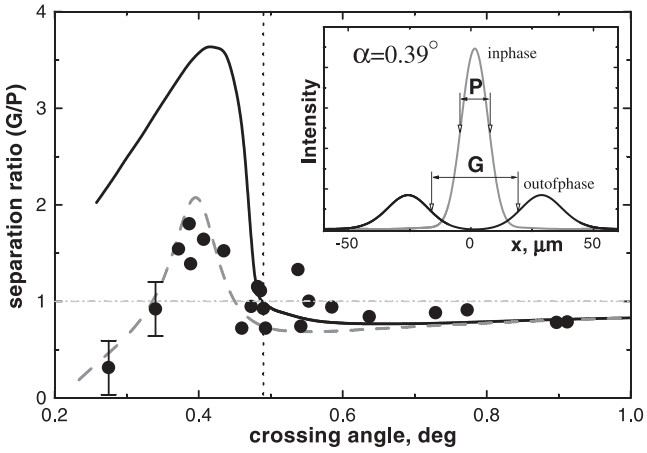

FIGURE 4 Separation between the two out-of-phase beams with respect to the width of the two in-phase beams: *dots*, experimental data; *solid line*, numerical results; *dashed line*, best fit; *vertical dashed line*, the critical angle for fusion. *Error bars* that account for the variation of the initial conditions are shown for lower crossing angles. *Inset*: numerically calculated beam cross-sections at the output face of the crystal for a crossing angle of 0.39°

phase beam is greatly elongated near the threshold leading to a decrease in the ratio $\boldsymbol{G/P}$.

The numerical results are in good agreement with the experiments, showing correctly the existence of a single maximum, and predicting the correct shape of the curve $\boldsymbol{G/P}$. The numerics, however, display a much higher contrast for the splitting ratio $\boldsymbol{G/P}$ with a maximal value ~ 3.6. This difference is attributed to the idealised conditions described by the model in (2).

Additionally we measured experimentally the power losses due to the collision of solitons with different relative phases. This power loss was estimated as the difference between the power transmission of a single beam and the power transmission when the two beams collide. The power transmission of a single soliton was estimated to be 83%, while the transmission for interacting beams depends on the crossing angle and the relative phase. The power loss for out-of-phase interacting beams varies from 8 to 18% for small to large crossing angles (for $\alpha \in [0.27–1.0°]$) respectively. For attracting beams the dependence is inverted. The losses for the in-phase interacting beams vary from 23 to 8%, respectively, for the fusion and non-fusion cases. The incoherently interacting beams exhibit similar but smaller losses – from 8 to 3% depending on whether the beams have fused or not. The above estimates show that a significant amount of the energy is lost in the interaction process. Beam fusion results in higher radiation losses compared with interactions in which no fusion occurs.

A practical realisation of optical switching is associated with the use of the solitons as information-carrying channels when the solitons guide and switch (information) optical beams at different wavelengths [32]. To demonstrate this feature we launched a red He-Ne laser beam (632.8 nm) into one of the waveguides. Both green beams cross each other at the angle for the maximum separation ratio ($\boldsymbol{G/P}$), $\alpha = 0.4°$. In Fig. 5 we show the images of the transmitted He-Ne laser beam for the cases in which the two soliton beams are out-of-phase (Fig. 5a) and in-phase (Fig. 5b). During switching,

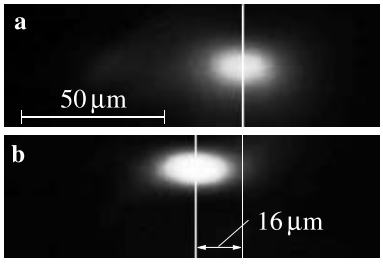

FIGURE 5 Images of the probe He-Ne laser beam for **a** out-of-phase green beams and **b** in-phase beams

the red beam is displaced by 16 μm from its original position. This shift, however, is smaller than the shift of the central part of the green beam for in- and out-of-phase interaction, which is 21 μm. This implies that the guiding properties of the formed waveguide structures are not perfect for the red beam. Additionally, part of the energy of the He-Ne laser beam is transferred to the other (left) channel when out-of-phase beams form a two channel output.

In general, varying the inter-beam interaction from attractive to repulsive offers a method for easy and reliable high contrast all-optical switching of probe beams.

6 Conclusion

In conclusion, we studied coherent and incoherent interactions of optical spatial solitons in a biased photorefractive crystal. By varying the intersection angle between initially overlapping beams we identified the existence of a clear threshold for the fusion of in-phase and mutually incoherent solitons. The critical angle for fusion of the in-phase beams was found to be higher than that for the incoherent ones, a result which agrees with the prediction of a simple waveguide model for soliton interaction in nonlinear media. We also investigated a use for the soliton fusion effect in optical switching. Our experimental results are in excellent agreement with numerical simulations of the full nonlinear model of photorefractive interaction and they represent generic properties of soliton interactions in other nonlinear media.

ACKNOWLEDGEMENTS J. Schröder acknowledges support by the German-Australian Cooperation Scheme by DAAD under Contract No. ppp 424. The work of G. McCarthy, D. Neshev and W. Krolikowski was supported by the Australian Research Council under the ARC Centres of Excellence program. CUDOS (the Centre for Ultrahigh bandwidth Devices for Optical Systems) is an ARC Centre of Excellence.

REFERENCES

1 G.I. Stegeman, M. Segev: Science **286**, 1518 (1999)
2 G.I. Stegeman, D.N. Christodoulides, M. Segev: IEEE J. Sel. Top. Quantum Electron. **6**, 1419 (2000)
3 Y.S. Kivshar, G. Agrawal: *Optical Solitons: From Fibers to Photonic Crystals* (Academic Press, San Diego 2003)
4 M. Nakazawa: 'Ultrafast Optical TDM Transmission with the Use of Novel Nonlinear Optical Fiber Devices'. In: *OSA Trends in Optics and Photonics (TOPS), Vol. 80, Nonlinear Guided Waves and Their Applications, OSA Technical Digest* (OSA, Washington 2002) p. NLTuC1-3
5 Y. Kivshar, G. Stegeman: Opt. Photon. News **13**, 59 (2002)
6 J.P. Robinson, D.R. Andersen: Opt. Comput. Process. **2**, 57 (1992)
7 S. Blair, K. Wagner: Appl. Opt. **39**, 6006 (2000)
8 M.H. Jakubowski, K. Steiglitz, R. Squier: Phys. Rev. E **58**, 6752 (1998)
9 A. Snyder, F. Ladouceur: Opt. Photon. News **10**, 35 (1999)
10 J. Oficjalski, I. Bialynicki-Birula: Acta Phys. Polon. A **9**, 759 (1978)

11 S. Cowan, R.H. Enns, S.S. Rangnekar, S. Sanghera: Can. J. Phys. **64**, 311 (1986)
12 S. Gatz, J. Herrmann: J. Opt. Soc. Am. B **14**, 1795 (1997)
13 A. Snyder, A. Sheppard: Opt. Lett. **18**, 482 (1991)
14 F. Reynaud, A. Barthelemy: Europhys. Lett. **12**, 401 (1990)
15 M. Shalaby, A. Barthelemy: Opt. Lett. **16**, 1472 (1992)
16 M. Shalaby, F. Reynaud, A. Barthelemy: Opt. Lett. **17**, 778 (1992)
17 J.S. Aitchison, A.M. Weiner, Y. Silberberg, D.E. Leaird, M.K. Oliver, J.L. Jackel, P.W. Smith: Opt. Lett. **16**, 15 (1991); J.S. Aitchison, A.M. Weiner, Y. Silberberg, D.E. Leaird, M.K. Oliver, J.L. Jackel, P.W. Smith: J. Opt. Soc. Am. B **8**, 1290 (1991)
18 V. Tikhonenko, J. Christou, B. Luther-Davies: Phys. Rev. Lett. **76**, 2698 (1996)
19 M. Segev, B. Crosigniani, A. Yariv, B. Fischer: Phys. Rev. Lett. **68**, 923 (1994)
20 M.D. Iturbe-Castillo, P.A. Marquez Aguilar, J.J. Sanchez-Mondragon, S. Stepanov, V. Vysloukh: Appl. Phys. Lett. **64**, 408 (1994)
21 W. Krolikowski, B. Luther-Davies, C. Denz: IEEE J. Quantum Electron. **QE-39**, 1 (2003)
22 H. Meng, G. Salamo, M.-F. Shih, M. Segev: Opt. Lett. **22**, 448 (1997)
23 G.S. Garcia-Quirino, M.D. Iturbe-Castillo, V.A. Vysloukh, J.J. Sanchez-Mondragon, S.I. Stepanov: Opt. Lett. **22**, 154 (1997)
24 W. Krolikowski, S. Holmstrom: Opt. Lett. **22**, 369 (1997)
25 M.-F. Shih, M. Segev: Opt. Lett. **21**, 1538 (1996)
26 D. Kip, C. Herden, M. Wesner: Ferroelectr. **274**, 135 (2002)
27 A.V. Mamaev, M. Saffman, A.A. Zozulya: J. Opt. Soc. Am. B **15**, 2079 (1998)
28 P. Gunter, J.-P. Huignard (Eds.): *Topics in Applied Physics, Vols. 61/62, Photorefractive Materials and Their Applications I, II* (Springer-Verlag, Berlin 1988)
29 See, e.g., A.A. Zozulya, D.Z. Anderson: Phys. Rev. A **51**, 1520 (1995); A. Stepken, M.R. Beliĉ, F. Kaiser, W. Krolikowski, B. Luther-Davies: Phys. Rev. Lett. **82**, 540 (1999)
30 W. Krolikowski, M. Saffman, B. Luther-Davies, C. Denz: Phys. Rev. Lett. **80**, 3240 (1998)
31 A. Snyder, J. Love: *Optical Waveguide Theory* (Chapman and Hall, London 1983)
32 R. de la Fuente, A. Barthelemy, C. Froehly: Opt. Lett. **16**, 793 (1991); B. Luther-Davies, X. Yang: Opt. Lett. **17**, 496 (1992); J. Petter, C. Denz: Opt. Commun. **188**, 55 (2001)